Dielectric Image Lines*

S. P. SCHLESINGER† AND D. D. KING‡

Summary—**Some further studies on the dielectric image line are presented. Following a verification of field purity for the conventional image system, the effects of dielectric constant and dielectric geometry on loss, dispersion, and field extent are examined. Results are also discussed for an asymmetric line, *i.e.*, the case of dielectric binding medium partially submerged in an image surface.**

Introduction

IT IS the purpose of this paper to report further on the properties of one type of surface wave line, namely the dielectric image line.[1–5]

The axial propagation of electromagnetic energy, radially symmetric about a conducting or dielectric binding medium, has been investigated and reported on by many authors.[6–17] These lines may be thought of as "free" surface wave lines, as contrasted to a transmission line whose electromagnetic field is confined.

To overcome some of the objections of the completely free surface wave lines, one of the authors has developed a modified line which uses a half round dielectric rod mounted on an image plane.[1,2] The boundary conditions dictated by the presence of this plane support the existence of the desirable low-loss, no low frequency cut-off HE_{11} mode, but exclude the higher-loss undesirable modes of the E type. Thus a convenient supporting surface defines, and partially confines, the surrounding field. By choosing a reasonable rod diameter to wavelength ratio, a fairly loosely bound field with attendant low loss may be realized.[4] In addition, the conducting sheet acts as a polarization anchor, and reduces the mode conversion problem. Various circuit components such as bends, junctions, and launchers have been developed for image lines.[3]

Following a verification of field purity, the effect of dielectric constant and guiding surface geometry on the basic properties of the dielectric image line are discussed. These basic properties include loss, field extent, and dispersion. Given a conducting plane upon which a dielectric of some arbitrary cross section may be mounted, one recognizes two general possibilities: the dielectric may be mounted so that the plane is an image in a true sense, or part of the dielectric may be recessed into the conducting plane, producing what may be termed an asymmetrical image system. Both cases will be treated here.

Field Purity

The basic equations for round dielectric rod are rereviewed in the Appendix. The characteristic equation involving the radial parameters p and q and evolving out of the application of boundary conditions (3) was solved with $n=m=1$ for a broad range of dielectric constant. These results are shown in Figs. 1 and 2.

The field purity of the HE_{11} mode with a half round dielectric and image surface was substantiated experimentally. Fig. 3 shows a comparison between the radial decrement of axial field component as predicted from the basic equations for the full round rod, and the measured axial field distribution for several half round polystyrene rods mounted on an image surface. The measurements were made at 3 cm in an open resonator[4] with the E-field sensing probe mounted on one end wall and moved normal to the image surface. A thin slot in the end wall so arranged produces no field perturbation since for the HE_{11} mode only H_ϕ is present at $\phi=0$.

Effect of Dielectric Constant

The effect of dielectric constant on loss, field extent, and dispersion has received some attention in the litera-

* Manuscript received by the PGMTT, November 12, 1957; revised manuscript received, March 17, 1958. The work reported on herein was accomplished at The Johns Hopkins University, supported by AF Cambridge Res. Ctr.

† Dept. of Elec. Eng., Columbia University, New York, N. Y.
‡ Electronic Communications Inc., Timonium, Md.

[1] D. D. King, "Dielectric image line," *J. Appl. Phys.*, vol. 23, pp. 699–700; June, 1952.
[2] ——, "Properties of dielectric image lines," IRE TRANS. ON MICROWAVE THEORY AND TECHNIQUES, vol. MTT-3, pp. 75–81; March, 1955.
[3] ——, "Circuit components in dielectric image lines," IRE TRANS. ON MICROWAVE THEORY AND TECHNIQUES, vol. MTT-3, pp. 35–39; December, 1955.
[4] D. D. King and S. P. Schlesinger, "Losses in dielectric image lines," IRE TRANS. ON MICROWAVE THEORY AND TECHNIQUES, vol. MTT-5, pp. 31–35; January, 1957.
[5] S. P. Schlesinger and D. D. King, "Some Fundamental Properties of Dielectric Image Line," Rad. Lab., The Johns Hopkins University, Baltimore, Md., Final Rep. AFCRC-TN-56-766; December, 1956.
[6] A. Sommerfeld, "Über die fortplanzung Elektrodynamischer Wellen langes eines Drahtes," *Ann. Phys. Chem.*, vol. 67, p. 233; July, 1899.
[7] G. Goubau, "Surface waves and their application to transmission lines," *J. Appl. Phys.*, vol. 21, pp. 1119–1128; November, 1950.
[8] H. M. Barlow and A. E. Karbowiak, "An investigation of the characteristics of cylindrical surface waves," *Proc. IEE*, vol. 100, pt. 3, pp. 321–328; November, 1953.
[9] E. H. Sheibe, B. G. King, and D. L. Van Zeeland, "Loss measurements of surface wave transmission lines," *J. Appl. Phys.*, vol. 25, pp. 790–797; June, 1954.
[10] D. Hondros and P. Debye, "Electromagnetische Wellen in dielektrischen Drahtes," *Ann. Phys.*, vol. 32, pp. 465–476; June, 1910.
[11] H. Ruter and O. Schriever, "Elektromagnetische Wellen an dielektrischen Drahten," *Schrift. Naturalwiss. Ver. Schleswig-Holstein*, vol. 16, pp. 2–60; January, 1915.
[12] J. R. Carson, J. P. Mead, and S. A. Schelkunoff, "Hyperfrequency wave guide mathematical theory," *Bell Sys. Tech. J.*, vol. 15, pp. 310–333; April, 1936.
[13] R. E. Beam, M. M. Astrahan, W. C. Jakes, H. M. Wachowski, and W. L. Firestone, "Dielectric Tube Waveguides," Northwestern University, Evanston, Ill., Rep. ATI 94929, ch. 5; 1949.
[14] C. H. Chandler, "An investigation of dielectric rod as wave guide," *J. Appl. Phys.*, vol. 20, pp. 1188–1193; December, 1949.
[15] W. M. Elsasser, "Attenuation in a dielectric circular rod," *J. Appl. Phys.*, vol. 20, pp. 1193–1200; December, 1949.
[16] P. Mallach, "Untersuchungen an dielektrischen wellenleitern in Stab- und Rohrform," *FTZ*, vol. 1, pp. 8–13; Heft 1, 1955.
[17] H. G. Unger, "Übertragungswerte von Wellen an dielektrischen Leitern," *FTZ*, vol. 8, pp. 438–443; Heft 8, 1955.

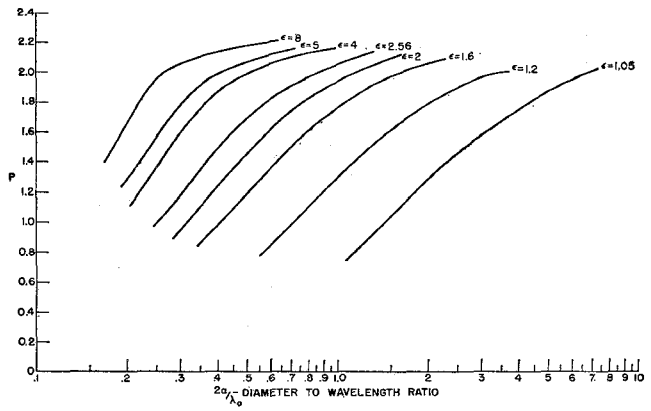

Fig. 1—Radial parameter p as a function of $2a/\lambda_0$ for round rod of dielectric constant ϵ.

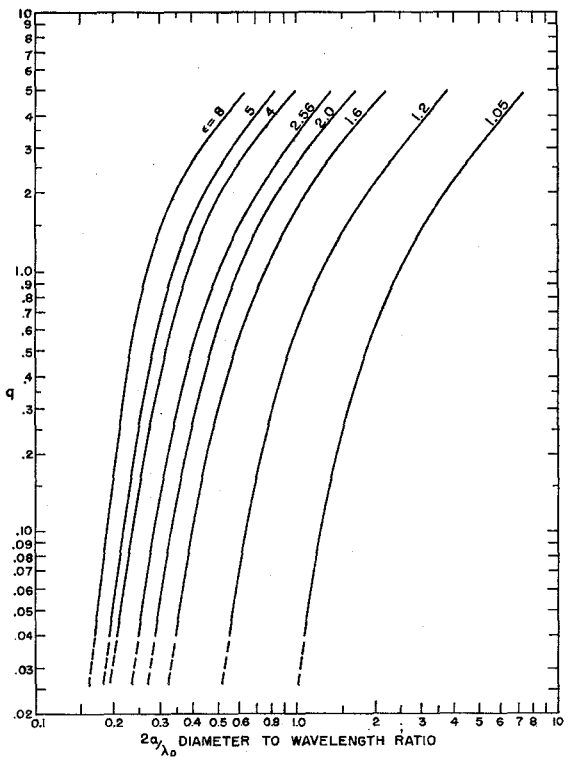

Fig. 2—Radial parameter q as a function of $2a/\lambda_0$ for round rod of dielectric constant ϵ.

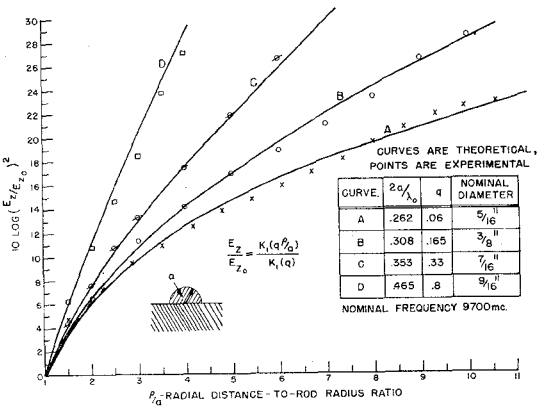

Fig. 3—The radial field distribution at $\phi=0$ showing the predicted and measured decrement of field in db for four samples of half round dielectric rod ($\epsilon=2.56$).

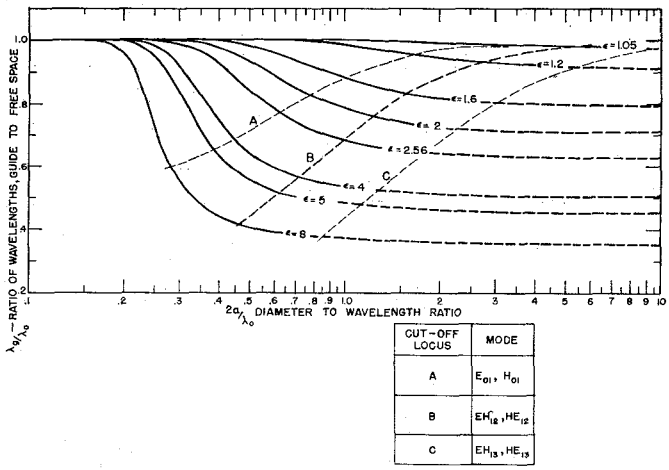

Fig. 4—Effect of dielectric constant on the dispersion characteristics of round rod.

ture[16,17] but the range of dielectric constant considered is rather limited, and the results are not presented in a form so as to show the over-all effect of ϵ on field binding and loss in one composite curve. The authors have calculated rod characteristics for a rather broad range of ϵ, based upon the solution of the characteristic equation for the HE_{11} mode.

The effect of dielectric constant on dispersive properties of a dielectric rod propagating the HE_{11} mode may be determined by using in (5) the p, q pairs that satisfy (3). This results in the curves shown in Fig. 4. Note that wavelength approaches asymptotically the value intrinsic in the medium.

The line loss for a half round dielectric rod on an infinite image surface consists of both dielectric loss and the image plane conduction loss. The authors have derived and experimentally confirmed the expression giving the conduction loss for the dielectric image line propagating the HE_{11} mode.[4] The dielectric loss for the full round rod for this case of $n=m=1$ was determined by Chandler and Elsasser.[14,15] For completeness both of these results are summarized in the Appendix. The loss functions R and R', complex functions of the system parameters, have been calculated for various values of ϵ as shown in Figs. 5 and 6.

Fig. 7 shows a family of curves showing the effect of giving dielectric constant on dielectric loss at 9700 mc and for an assumed loss tangent of 0.001. (The image plane conduction loss, α_c, has been shown to remain an order of magnitude less than α_d for reasonable values of $2a/\lambda_0$ and for wavelengths well into the millimeter region.[4] Fig. 7 shows that α_d tends to peak sharply for high dielectric constant, with no gradual transition toward a maximum. This can be attributed to the short intrinsic wavelength within the rod, which provides very effective binding. As the rod size increases, a lower average field

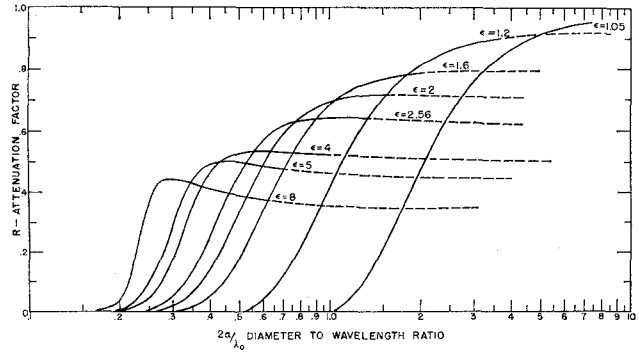

Fig. 5—Dielectric attenuation factor R as a function of $2a/\lambda_0$ for various values of ϵ.

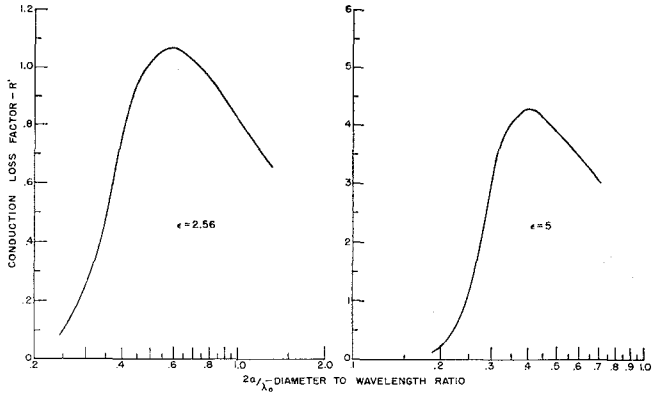

Fig. 6—Conduction attenuation factor R' as a function of $2a/\lambda_0$ for $\epsilon=2.56$, and $\epsilon=5$.

density of the larger cross section reduces the loss.

Since all the pertinent parameters are calculated for the HE_{11} mode and are on hand it would seem valuable to construct a universal plot, showing the combined effect of ϵ on loss, field spread, and rod size, all normalized for frequency and loss tangent. Fig. 8 is such a plot. Here we have a dimensionless loss factor, $\mathfrak{L}=\alpha_d\lambda_0/\phi$ shown as a function of ϵ with field extent ρ_L/λ_0 and rod size $2a/\lambda_0$, as convenient parameters.

The ρ_L of Fig. 8 defines the "extent of field" and is that radius at which the axial field density has decreased by 20 db. This larger value was chosen in preference to the e^{-1} decrease proposed by Mallach[16] since it places less burden on precise measurement of small attenuations.

Fig. 8 shows that for a given size rod and constant λ_0 a greater dielectric constant results in higher loss and closer binding. If we keep field extent constant and increase ϵ, the loss will go down. We note in addition the fact that for high values of ϵ, a change of 0.1 wavelength in diameter will give a much larger increment of loss than at low values of ϵ. This is important for broadband applications.

Effect of Dielectric Rod Configuration

A dielectric image line resonator with provision for axial field and guide wavelength measurement was used

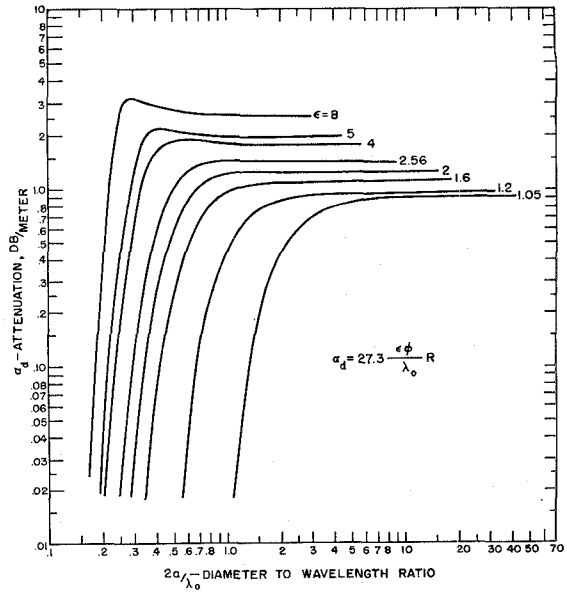

Fig. 7—Attenuation db/meter vs $2a/\lambda_0$ for various values of ϵ at 3 cm.

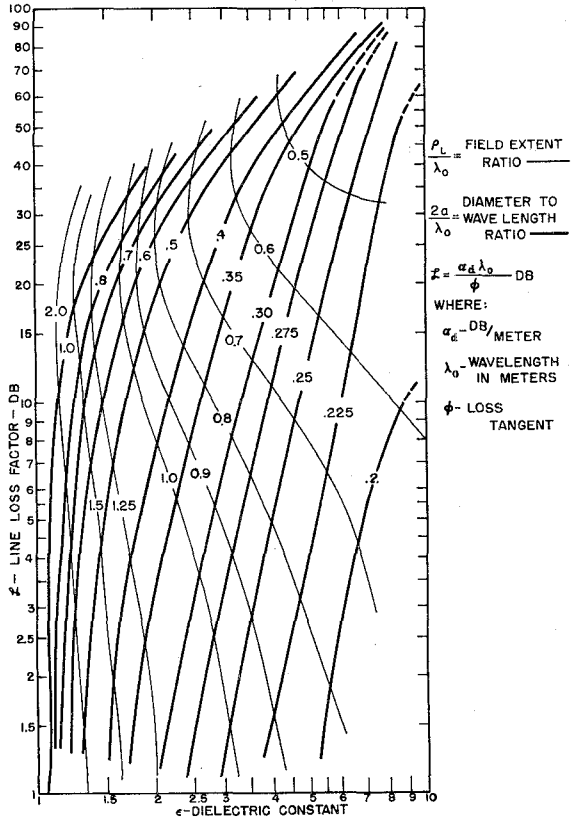

Fig. 8—Normalized line loss factor, $\mathfrak{L}$, as function of ϵ for constant $2a/\lambda_0$ and ρ_L/λ_0.

to measure the characteristics of a variety of dielectric cross sections (Fig. 9). We consider now some experimental data for these various dielectric configurations.

First we consider structures lying on the image plane, and thus the results may be applied to the free space full cross section by the theory of images. Secondly we

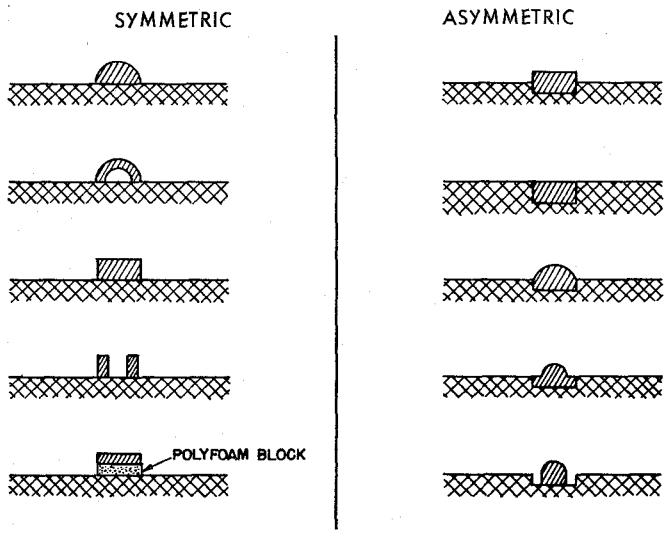

Fig. 9—Configurations of dielectric cross section.

consider the properties of a dielectric strip when partially submerged into a trench in the conducting plane. This produces an "asymmetrical image line"; the conducting sheet serves to perturb the field distribution within the rod because of the new boundary conditions, but no longer acts to mirror truly the configuration of field.

Generally, only field extent and propagation velocity properties are discussed, although the results of two actual measurements of line loss are reported—one for the symmetrical image and the other for the asymmetric or "trench line" case.

The True Image

The properties of the dielectric image line with a half round tube or rod have already been explored in terms of the properties of the full round structure.[13–15] These results may be summarized by noting that the dielectric tube is more attractive than the solid rod from the standpoint of loss and dispersion, but is somewhat less attractive with respect to field spread and ease of fabrication.

In choosing a cross section with which to work, we seek one that is easy to fabricate, lends itself conveniently to the asymmetrical case, and shows promise in binding the field. The rectangular dielectric rod meets these requirements.

The use of some relative field binding index is desirable for an arbitrary cross section. We define a binding effectiveness η_1 as the ratio of the field radius for a half round rod of the same material and cross sectional area as the sample considered to the field radius of that sample. Thus, $\eta_1 > 1$ indicates that the given material and transverse configuration binds closer than the same amount of material in a half round. It is also of interest to establish an index which serves as a guide to loss

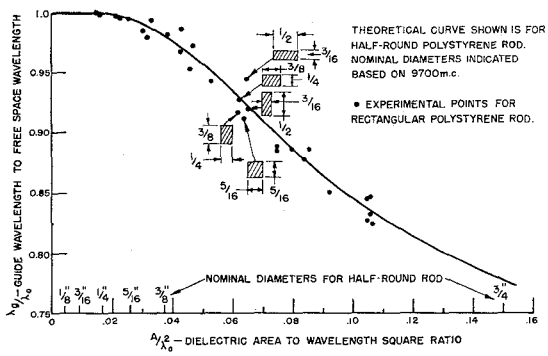

Fig. 10—Dependence of λ_g/λ_0 on the area of dielectric rod. Theoretical curve is for the half round rod; experimental points, for rectangular rod.

properties. We define η_2, the loss index, as the ratio of sample cross sectional area to the area of the half round rod of the same field extent and material.

Rectangular rod: The field extent and guide wavelength characteristics of seventeen samples of rectangular polystyrene rod were measured using the flat plate resonator. In each case the counted number of half-wavelengths yielded a value for λ_g for three or four neighboring resonances, following which a careful measurement was made of the radial distribution of axial electric field component. The latter data when plotted against radial distance-to-sample height ratio gave a 20-db field radius.

Dispersion: The mathematical solution for the circular dielectric as already outlined yields a convenient relation between guide to free space wavelength and the single principal dimension, diameter, provided that the diameter is expressed in number of wavelengths. Thus with a given rod size, the λ_g/λ_0 characteristics may be determined as a function of frequency, or given the frequency the variation with size may be obtained.

Several attempts were made to find a single controlling dimension for the rectangular rod, with the final result based on the intuitively evident fact that the propagation properties should depend on the area of dielectric. Fig. 10 shows how λ_g/λ_0 may be represented as almost a single curve when plotted against the area in square wavelengths. The curve actually drawn is for a half round polystyrene rod. We note that propagation velocity for the rectangular cross section is within about 3 per cent of the value for a half round rod of the same area and dielectric constant. We see further that given a certain area, the orientation has only a slight effect within the approximate 3 per cent.

In the interest of clarity of presentation, the three or four resonances read for each sample are not plotted in the figure, nor is each point identified. The points are not scattered, but if connected keeping either a or b constant, they would produce a closely bunched family of curves.

Fig. 11 shows four of these curves plotted, including

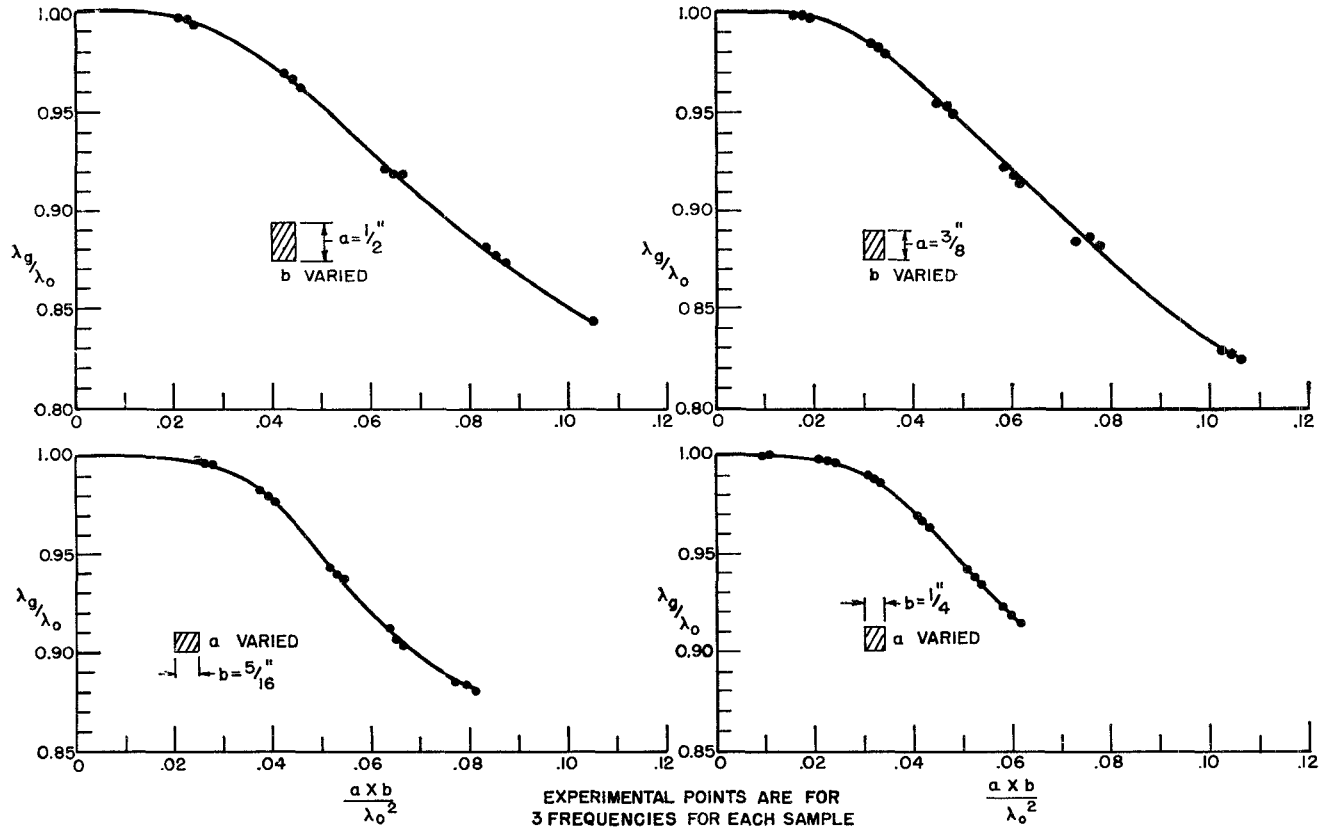

Fig. 11—The variation of λ_g/λ_0 with dielectric area in number of square wavelengths for four sets of rectangular rods.

the neighboring frequency points, indicating that A/λ_0^2 is a good approximation for a normalizing dimensionless ratio.

Field extent: The data representing field extent may be plotted in several different ways to examine the effect of varying each parameter. Attempts to correlate the field extent of rectangular rods with circular rods in terms of equivalent dimensions met with no success. It was noted, however, that the radial field distribution more closely approximated a Hankel function at larger distances, which is what would be expected considering that it is only close to the rectangular boundary that a perturbation on radial symmetry will exist.

The most satisfactory method of showing the results is illustrated in Fig. 12 where the field radius is plotted as a function of sample width for various values of height. There are a few important facts to be gained from this family of curves. The first thing to be noted is the evidence of a resonant effect, resulting in a loosening of the field where the width of sample approaches 3/8 inch ($b/\lambda_0 \approx 0.3$); this dimension very closely approximates the half-wavelength at 9700 mc intrinsic in the medium $\epsilon = 2.56$. This suggests the possibility of a transverse resonance with perhaps a null in the vicinity of $\phi = 0$. The 1/4-inch wide sample shows a particularly close binding.

If we examine the effect of the width dimension on binding quality by plotting the binding effectiveness η_1, we get the curves shown in Fig. 13. In addition to confirming the relatively good binding of the 1/4-inch wide sample, the curves show a surprising regularity considering the rather arbitrary manner of defining the ordinate. To summarize the significance of Fig. 13 we might say that given a sample of dielectric, there exist several sizes of rectangular configuration which are at least as effective in binding as the equivalent half round rod of the same area. The trend of η_2 leads to a similar generalization, as regards a qualitative loss comparison.

Miscellaneous shapes: The main objection to the use of half round dielectric tubing on an image plane lies in the difficulties involved in fabrication and mounting. Perhaps some more convenient transverse arrangement of dielectric mass would simulate physically a hollow tube, thus providing for a low-loss, moderately binding substitute.

In an attempt to realize the above, a pair of long thin rods were erected on the image plane in a manner quite like a pair of tracks. (See Fig. 9.) Measurements were taken on a set of rectangular rods each 3/16-inch high by 1/16-inch thick mounted on the image surface at various distances apart. From all appearances, guide wavelength, and nonradiating field extent, the tracks were propagating an HE_{11}-like mode. Another arrangement was tried whereby a 3/8-inch wide by 1/8-inch

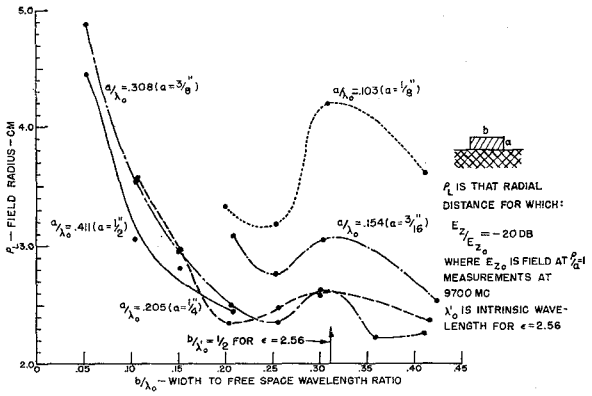

Fig. 12—Field radius, ρ_L vs b/λ_0 for rectangular rod of fixed a/λ_0. $\epsilon=2.5$, $\lambda_0=3.1$ cm.

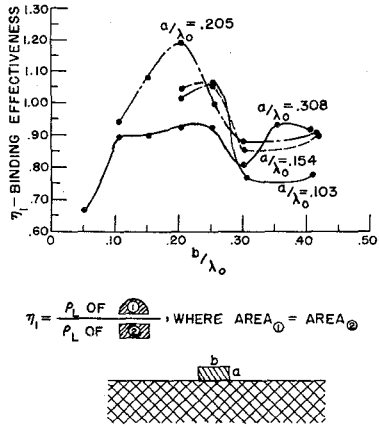

Fig. 13—Binding effectiveness as a function of b/λ_0 for rectangular rod of fixed a/λ_0. $\epsilon=2.5$, $\lambda_0=3$ cm.

thick dielectric slab was mounted above the image surface at various heights supported by polyfoam blocks (Fig. 9). These attempts to improve field binding compared to the same volume of dielectric formed as a tube, were unsuccessful although the dipole mode was easily established.

The properties of these configurations were not investigated further. It does seem that one advantage of a track line would be the ease with which field binding may be controlled. Thus in making slight bends in the horizontal plane one could minimize radiation by bringing the tracks together. This is most applicable at millimeter wavelengths where field spread in terms of many wavelengths is a reasonable value, thus making it possible for one to start with widely spaced strips.

The Asymmetrical Image

The presence of a convenient conducting surface upon which to mount various dielectric samples leads to the consideration of an interesting question. What would be the effect of gradually lowering a dielectric rod of some convenient cross section transmitting with an HE_{11}-like mode, into an axial slot, or trench cut into the conducting surface? Possibly, the change in field configuration brought about by the new boundary conditions within the dielectric, a region of high electric flux density, may result in an improvement in binding or loss for the resulting transmission line. The set of rectangular rods already used may be conveniently utilized for an analysis of this type. Fig. 9 illustrates the various configurations studied.

The dielectric image line resonator was reconstructed to provide a means of mounting the dielectric at various depths. A 3/8-inch wide, 7/16-inch groove was milled down the center of the conductor surface, and by the insertion of suitable long axial inserts, the dimensions of the trench could be varied. Due care was taken to insure conductivity continuity by the application of conducting silver filler to the joints created.

Rectangular rod: Runs were made on three widths of dielectric rectangular rod of various heights, lowered into the image plane to a depth of 1/16, 1/8, and 3/16 inch. In addition, a miscellaneous set of runs was conducted including the odd geometries shown in Fig. 9, plus a few measurements made on the full depth 7/16-inch trough filled with dielectric material. In each case it was possible to set up the HE_{11} mode, although for certain arrangements the binding was too loose to be practical.

Once again there are many ways that the available data could be plotted. One arrangement of these data shows that as a given size rod ($a+d$ is constant) is lowered into the image plane, the field becomes more and more loosely bound. (See Fig. 14 for dimensions a, b, d.) A more interesting consideration might be the following: given a rectangular configuration, what would be the effect on field spread and binding effectiveness of adding a base of ever-increasing depth submerged beneath the image surface?

Fig. 14, showing the field spread for three rectangular rods of different widths, indicates an appreciable tightening of field only for the case of the 3/8-inch rod. Recalling that this width sample operating on the plane showed symptoms of a transverse resonance of 9700 mc, (see Fig. 12), we may explain the apparent improvement in terms of a destroying of this condition for transverse resonance, by the substitution of a short circuit for the open circuit that existed at the side walls of the rod for the completely symmetrical case ($d=0$). This is further substantiated by Fig. 15 which shows an improvement in the binding effectiveness coefficient for the 3/8-inch wide rod sample; however, the coefficient never quite reaches unity.

We observe further from Fig. 14 that a 1/4-inch wide rectangular rod with heights of 1/8 and 3/16 inch does show some decrease in field extent when provided with a submerged base of 1/16-inch depth. The rod with the height of 1/8 inch is perhaps worthy of note since, as shown in Fig. 15, there results a 10 per cent increase in binding effectiveness.

In an effort to check this apparent high efficiency indicated in the latter case, two actual line loss measurements were made by methods described elsewhere,[4] for

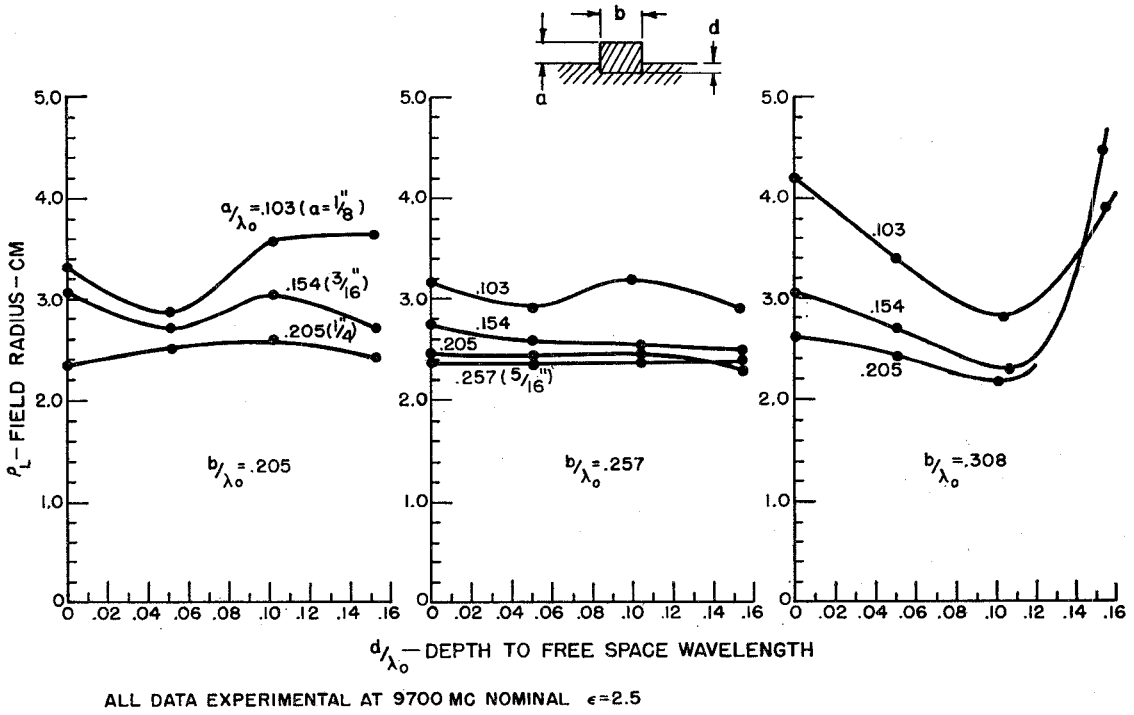

Fig. 14—The variation of field radius ρ_L with depth to free-space wavelength d/λ_0 for rectangular samples of various widths b/λ_0 and heights a/λ_0. $\epsilon = 2.5$, $\lambda_0 = 3.1$ cm.

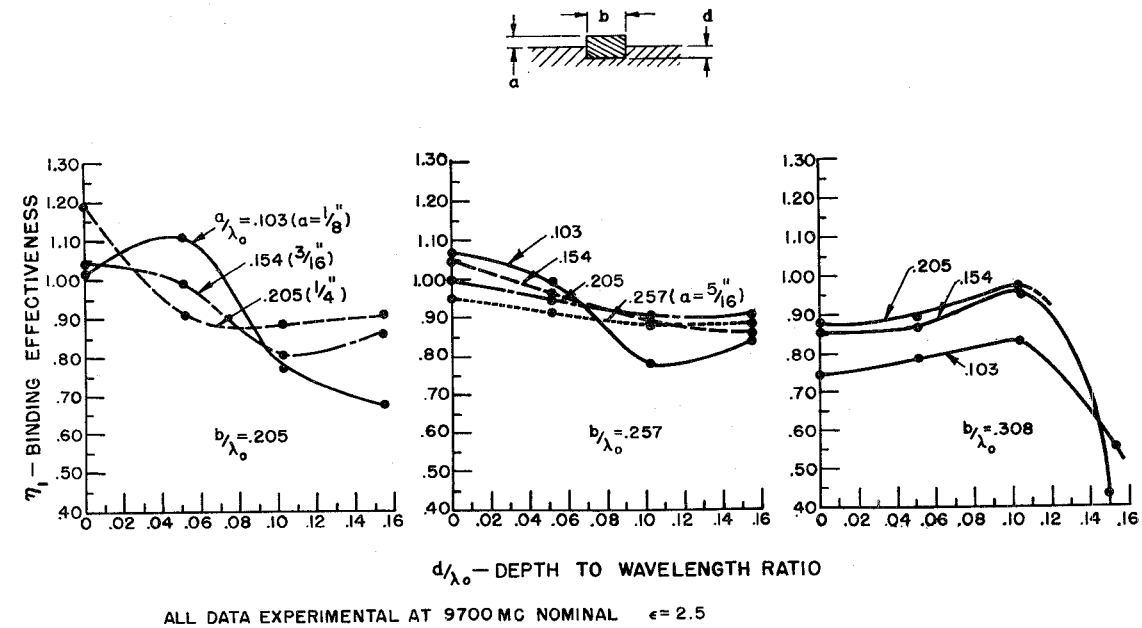

Fig. 15—Binding effectiveness, η_1, as a function of depth, d/λ_0, for various widths b/λ_0 and heights a/λ_0. $\epsilon = 2.5$, $\lambda_0 = 3.1$ cm.

the 1/4×1/8-inch rod, with and without the 1/16-inch submerged floor. The results of this measurement are shown in Fig. 16, where a decrease in loss of some 30 per cent is indicated for the dielectric rod with more mass mounted asymmetrically, compared to the smaller size rod with the same upper configuration mounted on the image surface. In addition we note the surprising fact that the lower loss sample has the more tightly bound field by about 20 per cent (see Fig. 14).

A complete set of curves was made showing the λ_g/λ_0 ratio as a function of area, expressed in number of square wavelengths. These curves are not given here because the results showed in each case that the dispersive properties of the rectangular rod dielectric image trench line remain essentially independent of the depth of penetration into the image plane for binding medium of constant height a. In other words if we plot all the results for the asymmetrical case using directly the set

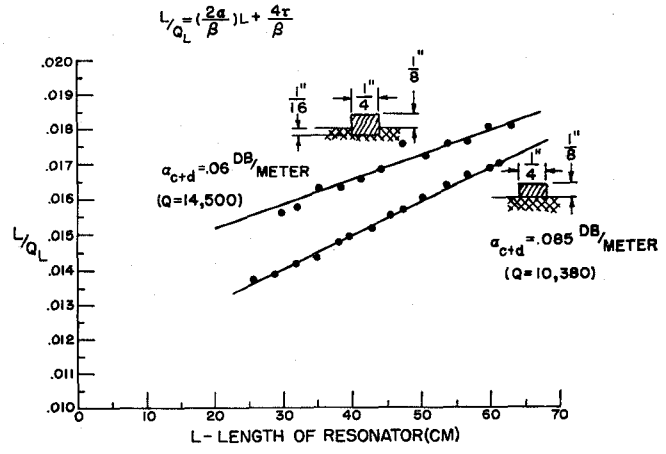

Fig. 16—Experimental curves for separating line loss from miscellaneous end losses, L/Q_L vs L, for a symmetric and an asymmetric dielectric image line with rectangular dielectric as binding medium. $\epsilon=2.56$, $\lambda_0=3.1$ cm.

of axes of Fig. 10 with depth as a parameter, the curves will all lie within the aforementioned 3 per cent of the expected value for a half round rod of equal area. This is true for the 1/4-inch wide samples and holds also to a lesser extent for the 3/8-inch wide samples, even though the added area beneath the surface resulted in a closer field binding.

Miscellaneous shapes: The properties of various odd shapes (Fig. 9) were measured, but the results will not be given in detail since the characteristics followed the same general trend as described in the last section for the rectangular rod asymmetrical image line. For example, the binding properties of a small semicircular rod were not enhanced by the presence of the buried rectangular base, whereas the larger size rods showed some improvement for small bases, but generally the improvement was not spectacular.

The case of a full 7/16-inch deep trench filled with polystyrene rod was investigated.[18] For two widths, 1/4 and 3/8 inch, the simultaneous existence was noted of a closely bound low-Q trench mode of propagation and a high-Q, loosely bound nonradiating HE_{11}-like dipole mode. Taking advantage of the inherently different guide wavelengths, it was a simple matter to utilize the resonator as a mode filter.

Conclusions

The dielectric image line consisting of a half round dielectric rod mounted on a conducting surface of infinite extent propagates the nonradiating HE_{11} mode with a field distribution as predicted from the symmetry of the defining equations and confirmed experimentally, that is, identical to the free-space dielectric transmission line. The presence of the image surface provides for support and limits the contaminating modes to the H type.

[18] F. J. Zucker, "The guiding and radiation of surface waves," *Proc. Symp. on Modern Advances in Microwave Techniques*, Polytechnic Inst. of Brooklyn, Brooklyn, N. Y., vol. 4; 1954.

An evaluation of a loss factor $\mathfrak{L}$ for a broad range of values of the dielectric constant ϵ suggests that low losses and reasonable extent of field may be realized by the fabrication of the binding medium using a material of low dielectric constant. This is particularly desirable at millimeter wavelengths since the increased size of rod for a given set of properties makes handling and fabrication more convenient.

Although there is evidence of a resonance for a transverse dimension approaching intrinsic half wavelength, there are a few sizes of rectangular dielectric rod which may be used as the binding medium for a dielectric image line with resulting increase in binding and loss effectiveness. The guide wavelength for a line with this configuration of cross section is within about 3 per cent of the value for a half round rod of the same area and dielectric constant.

The possibility of efficient surface wave transmission by means of an asymmetrical image system has been examined. The results were not conclusive. For one case, a rectangular "trench line" with the dielectric partially submerged into the image sheet, propagated the HE_{11} mode with lower loss and closer binding than a symmetrical rectangular line with a dielectric having the same area above the plane.

Appendix

Basic Equations for Dielectric Rod

We assume axial field variations in dielectric mediums 1 and 2 as follows:

$$\begin{aligned} E_{z_1} &= AJ_n(p\rho/a)\cos n\phi \\ H_{z_1} &= BJ_n(p\rho/a)\sin n\phi \\ E_{z_2} &= CK_n(q\rho/a)\cos n\phi \\ H_{z_2} &= DK_n(q\rho/a)\sin n\phi \end{aligned} \tag{1}$$

where

$$\begin{aligned} K_{c_1}^2 &= (p/a)^2 = \omega^2\mu\epsilon_1 - \beta^2 \\ K_{c_2}^2 &= (jq/a)^2 = \omega^2\mu\epsilon_2 - \beta^2. \end{aligned} \tag{2}$$

Determination of the other field components in the usual manner followed by the application of boundary conditions at the rod surface, $\rho=a$, yields finally:

$$(f+g)(\epsilon f+g) - n^2(1/q^2+\epsilon/p^2)(1/p^2+1/q^2) = 0 \tag{3}$$

where

$$f=\frac{J_n'(p)}{pJ_n(p)} \quad \text{and} \quad g=\frac{K_n'(q)}{qK_n(q)}.$$

Two additional expressions may be derived; these are:

$$2a/\lambda_0 = 1/\pi\left(\frac{p^2+q^2}{\epsilon-1}\right)^{1/2} \tag{4}$$

$$\lambda_g/\lambda_0 = \left(\frac{p^2+q^2}{p^2+\epsilon q^2}\right)^{1/2}. \tag{5}$$

Image Line Loss

The total line loss for the dielectric image line in nepers/meter is given as:

$$\alpha' = \frac{1}{2}\frac{\sum_{i=1,2} 2R_s \int_{0,a}^{a,\infty} |\hat{n}\times \boldsymbol{H}_i|^2 d\rho\Big|_{\phi=\pi/2} + \sigma_d \int_0^a \int_{-\pi/2}^{\pi/2} |E_1|^2 \rho d\rho d\phi}{\sum_{i=1,2} \int_{0,a}^{a,\infty} \int_{-\pi/2}^{\pi/2} |\boldsymbol{E}_i \times \boldsymbol{H}_i| \rho d\rho d\phi}$$

or finally

$$\alpha = 69.5\left(\frac{R_s}{\zeta_2 \lambda_0}\right) R' + 27.3\left(\frac{\epsilon \phi_d}{\lambda_0}\right) R$$

where

α = line loss db/meter,
ϕ_d = loss tangent of dielectric rod,
R_s = image surface resistance,
$\zeta_2 = \sqrt{\mu_2/\epsilon_2} = \sqrt{\mu_0/\epsilon_0}$,
λ_0 = free-space wavelength, meters,
σ_d = conductivity of dielectric rod.

The functions R and R' are defined as:

$$R = \frac{N}{D}$$

$$R' = \frac{1}{\pi \frac{2a}{\lambda_0} D}\left[\frac{f(I_1 I_0)}{J_1^2(p)} + \frac{f(H_1 H_0)}{K_1^2(q)}\right]$$

$$N = \left[\frac{\mu\epsilon - 1}{q^2}\left\{\frac{f^2 + \frac{1}{p^2} - \frac{1}{p^4}}{\frac{1}{p^2} + \frac{1}{q^2}}\right\} + (\mu V^2 + U^2)X + \frac{4\mu UV}{p^4}\right]$$

$$D = \left[UX(\epsilon + \mu V^2) + UY(1 + V^2) + \frac{2V}{p^4}(\mu\epsilon + U^2) - \frac{2V(1 + U^2)}{q^4}\right]$$

$$U = \frac{\lambda_0}{\lambda_g}$$

$$V = \left[\frac{(\epsilon f + g)}{(\mu f + g)}\right]^{1/2}$$

$$X = f^2 + \frac{(2f + 1)}{p^2} - \frac{1}{p^4}$$

$$Y = -g - \frac{(2g - 1)}{q^2} + \frac{1}{q^4}$$

$$f(I_1 I_0) = \frac{2}{3}\epsilon^2 \frac{S(2S + 3)}{p^3}\{I_1 + J_0(p)J_1(p)\} + I_1 \frac{V^2(\mu\epsilon - 1)}{p(p^2 + q^2)} - \frac{1}{3} I_0 \epsilon^2 \frac{(S^2 - 3)}{p^3} - \frac{1}{3}\epsilon^2 \frac{S^2}{p^4} J_1^2(p)$$

$$f(H_1 H_0) = -\frac{2}{3}\frac{T(2T + 3)}{q^3}\{H_1 + K_0(q)K_1(q)\} + H_1 \frac{V^2(\epsilon - 1)}{q(p^2 + q^2)} - \frac{1}{3} H_0 \frac{(T^2 - 3)}{q^3} - \frac{1}{3}\frac{T^2}{q^4} K_1^2(q)$$

$$S = \left(\frac{UV}{\epsilon} - 1\right)$$

$$T = (UV - 1)$$

$$I_1 = \int_0^p J_1^2(Z)dZ \qquad H_1 = \int_q^\infty K_1^2(Z)dZ$$

$$I_0 = \int_0^p J_0^2(Z)dZ \qquad H_0 = \int_q^\infty K_0^2(Z)dZ.$$